

MoEMba: A Mamba-based Mixture of Experts for High-Density EMG-based Hand Gesture Recognition

Mehran Shabanpour[†], Kasra Rad[†], Sadaf Khademi[†], and Arash Mohammadi[†]

Abstract—High-Density surface Electromyography (HD-sEMG) has emerged as a pivotal resource for Human-Computer Interaction (HCI), offering direct insights into muscle activities and motion intentions. However, a significant challenge in practical implementations of HD-sEMG-based models is the low accuracy of inter-session and inter-subject classification. Variability between sessions can reach up to 40% due to the inherent temporal variability of HD-sEMG signals. Targeting this challenge, the paper introduces the MoEMba framework, a novel approach leveraging Selective State-Space Models (SSMs) to enhance HD-sEMG-based gesture recognition. The MoEMba framework captures temporal dependencies and cross-channel interactions through channel attention techniques. Furthermore, wavelet feature modulation is integrated to capture multi-scale temporal and spatial relations, improving signal representation. Experimental results on the CapgMyo HD-sEMG dataset demonstrate that MoEMba achieves a balanced accuracy of 56.9%, outperforming its state-of-the-art counterparts. The proposed framework’s robustness to session-to-session variability and its efficient handling of high-dimensional multivariate time series data highlight its potential for advancing HD-sEMG-powered HCI systems.

Index Terms—Electromyography, Gesture Recognition, Mixture of Experts, State Space Models, Wavelet Decomposition.

I. INTRODUCTION

Surface ElectroMyoGraphy (sEMG) signals [1] are a promising resource for Human-Computer Interaction (HCI), providing direct insights into muscle activities due to their ability to encapsulate motion intentions [2]. As such, sEMG-based gesture recognition frameworks emerged as the core technology in developing cutting-edge Muscle-Computer Interfaces (MCIs), facilitating applications ranging from active prostheses [3]–[7], wheelchairs [8], [9] and exoskeletons [10], as well as in neuromuscular diagnosis [11], neurorehabilitation [12], and video game interactions [13]. Recent advancements in Artificial Intelligence (AI)-driven solutions have significantly enhanced the development of sEMG-powered MCIs. AI-based MCI tasks range from discrete movement classification and joint angle estimation to force/torque estimation offering significant potential to advance EMG pattern recognition. Despite the recent surge of interest, such models fail to address critical challenges faced in non-ideal, practical conditions, including variations in electrode placement and changes in muscle state both

across different subjects and within the same person over time [14], [15].

Literature Review: MCI systems commonly rely on a set of standardized functions to represent features from different domains, enhancing the information density embedded in high-density (HD)-sEMG signals, and improving the discrimination of different gestures. The extracted representations can be utilized for sEMG pattern recognition through various classifiers, which are broadly classified into two primary categories:

Machine Learning (ML)-based Methods [16]: ML models rely on feature engineering, where relevant features are designed and extracted manually from signals encompassing three primary categories: time-domain (TD), frequency-domain (FD), and time-frequency domain (TFD) features. TD features [6], [7] are derived directly from raw sEMG signals, representing their time-dependent variations, and are particularly beneficial due to their low computational complexity. In contrast, FD features [17] are obtained through the Fourier transform of the sEMG signal’s autocorrelation function. Building upon these approaches, TFD features [18] combine both time and frequency information, providing a comprehensive view of the signal’s energy distribution, with wavelet transform being a commonly used technique for this analysis. Despite the availability of various feature extraction techniques, the multidimensional, non-linear and multichannel nature of sEMG coupled with its inherent non-stationary nature, makes this signal challenging for effective training of ML models [19].

Deep Learning (DL)-driven Models [20]: DL, on the contrary, is distinguished by its hierarchical architecture. This structure enables the model to progressively extract complex feature representations, automatically capturing underlying patterns and relationships within the data at various levels. The capability of autonomously extracting spatial features made Convolutional Neural Networks (CNNs) [21], [22] a leading choice for sEMG gesture recognition in DL-driven models. However, limited receptive fields of CNNs restrict their ability to capture long-range dependencies in sEMG signals, which are inherently sequential time series data. In contrast, Recurrent Neural Networks (RNNs) [23], [24], designed specifically to model temporal relationships and sequential patterns, offer a more suitable approach for analyzing such signals. Consequently, several approaches utilize hybrid CNN-RNN models [19], [25]. This combined architecture excels in capturing both spatial and temporal features. On the other hand, transformers offer a compelling

This work was partially supported by the Natural Sciences and Engineering Research Council (NSERC) of Canada through the NSERC Discovery Grant RGPIN-2023-05654.

[†]All authors are with Concordia Institute for Information Systems Engineering (CIISE), Concordia University, Montreal, Canada.

alternative with their self-attention mechanism [26], [27], granting global receptive fields and enabling superior capture of cross-time dependencies, addressing the limitations of both CNNs and RNNs in this regard. This global perspective, while advantageous, is computationally expensive. The self-attention mechanism necessitates each element attend to all others, leading to computational overhead that scales quadratically with sequence length [25], [28].

Targeted Challenges: Although DL-driven models have achieved remarkable accuracies in intra-session tasks, their performance diminishes in inter-session and inter-subject scenarios [29], [30]. In the context of sEMG analysis, these terms describe distinct data collection paradigms: intra-session involves data from a single subject during a continuous recording, inter-session refers to recordings from the same subject across multiple sessions, and inter-subject pertains to data from different individuals.

In greater detail, a key challenge in practical implementations is the low accuracy of inter-session and inter-subject classification, with session-to-session variability reaching as high as 10–40%, which arises from the inherent temporal variability of sEMG signals. This variability is influenced by several factors, including muscle condition (fatigue, atrophy, or hypertrophy), changes in skin impedance (such as sweating), anatomical differences among subjects, non-stationarities due to limb positioning and force variations, and electrode drift, all of which contribute to accuracy degradation. Moreover, these factors can introduce considerable inconsistencies in signal patterns across different sessions and individuals, thus complicating the generalization of gesture recognition algorithms [20], [30]–[32].

The challenge of between-session distribution shifts has been conventionally handled through experimental design by developing multi-user and multi-session training protocols, as well as data processing techniques such as data augmentation [30], [31], unsupervised learning, and transfer learning [33], [34] with advanced DL architectures. Despite offering improvements in accuracy, these methods often require large amounts of adaptation data [28], [31], [35]. Moreover, sEMG data collection is a time-consuming and resource-intensive process [30], [35], requiring specialized equipment and trained personnel, which further limits the availability of data. Moreover, the significant computational demands of these methods restrict their feasibility for real-time applications, particularly in resource-constrained embedded systems [28], [31].

A key consideration, often overlooked in most above-mentioned models, is the inter-channel dependencies inherent in sEMG data. Gesture movements involve complex inter-muscular coordination, which is reflected in the inter-channel relationships captured by the placement of sEMG electrodes. Many models incorrectly apply a channel-independent approach, treating the data as uncorrelated univariate time series and thus neglecting these essential inter-channel relationships [25], [28], [33]. Although some approaches [36], [37] attempt to address this limitation by combining channels

using mechanisms such as self-attention, linear combinations, or convolutions, these methods are computationally expensive and generally miss proportional relationships by modeling inter-channel relationships as weighted sums.

Contributions: Recognizing the crucial role of cross-channel dependencies in multivariate time series, we aim to capture temporal dependencies in HD-sEMG signals using Selective State Spaces (SSS), and address cross-channel interactions through techniques of channel attention. Recent advancements in State-Space Models (SSMs) [28], notably Mamba, offer efficient modeling of sequential data dynamics with linear computational complexity without losing the global receptive field, even for long sequences, positioning them as a potential alternative to transformers. In other words, SSMs adopt an RNN-like approach that facilitate dynamic adaptation to data distribution shifts, enabling the capture of diverse temporal features such as long-term trends and short-term fluctuations.

The paper introduces the MoEMba framework built upon the Mamba architecture—a novel lightweight advanced SSM-based approach—specifically designed to address the critical challenge of session-to-session variability while prioritizing simplicity and efficiency. In summary, the paper makes the following contributions:

- As the first application of Mamba for HD-sEMG hand gesture recognition, MoEMba model uses an adaptive combination of multiple Mamba experts within a Mixture of Experts (MoE) configuration to capture both short-term and long-term gesture dynamics.
- Wavelet Transform Feature Modulation (WTFM) is incorporated to capture multi-scale temporal and between-channel spatial relations, integrating both time-domain and frequency-domain information to enhance signal representation.
- The MoEMba’s design, including its architecture and feature extraction, is computationally efficient requiring fewer Floating Point Operations per Second (FLOPS) than State-Of-The-Art (SOTA) models. This efficiency, combined with robustness to session-to-session variability in HD-sEMG recordings makes MoEMba ideal for real-world applications like prosthetic control and human-computer interaction.

The remainder of the paper is organized as follows: Section II begins by describing the dataset used in this research and provides an overview of the relevant background. Section III introduces our proposed framework, MoEMba, detailing its architecture and key components. Section IV presents a comprehensive analysis of the experimental results. Finally, Section V concludes the paper.

II. MATERIALS AND METHODS

In this section, first, we briefly present the HD-sEMG dataset used for development and testing of the MoEMba framework. Then, required background on State-Space Models (SSMs) is introduced.

A. Dataset

In this study, we used the CapgMyo HD-sEMG dataset [30], recorded from 128 channels sampled at 1000Hz. We utilized sub-databases DB-a (23 subjects performing 8 gestures held for 3 – 10s) and DB-b (a subset of DB-a comprising 10 subjects with recordings from two sessions separated by a minimum of 7 days, performing the same 8 gestures with hold durations of ~ 3 s). The CapgMyo HD-sEMG dataset configuration introduces inter-session and inter-subject variability, which challenge model robustness—an issue that this study aims to address. To capture richer semantic information and local features, the data was pre-processed using 45 – 55Hz Butterworth filter, followed by segmentation into overlapping 64ms windows with 8ms steps, resulting in 64×128 matrices, and finally normalized to $[-1, 1]$.

B. Selective State-Space Models

The SSMs are mathematical models used to represent dynamic systems through state variables [38]. Fundamentally, SSMs characterize the evolution of a system through two primary equations, i.e., the state model, and the observation model. The state model defines the evolution of the hidden state $h(t)$ over time as influenced by the input $x(t)$

$$h'(t) = Ah(t) + Bx(t), \quad (1)$$

where $A \in \mathbb{R}^{N \times N}$ is the state transition matrix, $B \in \mathbb{R}^{N \times 1}$ is the input matrix, $h(t) \in \mathbb{R}^N$ is the hidden state at time t , and $h'(t)$ is the derivative of the hidden state. This evolution of the hidden state is then used by the observation equation to determine the output $y(t)$

$$y(t) = Ch(t) + Dx(t), \quad (2)$$

where $C \in \mathbb{R}^{1 \times N}$ is the output matrix, and $D \in \mathbb{R}$ is the direct feedthrough term (often set to zero). The application of SSMs within ML context requires the discretization of the continuous-time formulations. A common discretization method is the Zero-Order Hold (ZOH), which assumes a constant function value over an interval. After ZOH discretization, the SSM equations can be rewritten as follows

$$h_k = \bar{A}h_{k-1} + \bar{B}x_k, \quad (3)$$

$$y_k = \bar{C}h_k, \quad (4)$$

where $\bar{A} = \exp(\Delta A)$, and $\bar{B} = (\Delta A)^{-1}(\exp(\Delta A) - \mathbf{I})B$. Furthermore, h_k is the hidden state at discrete time step k , x_k and y_k represent the input and output at discrete time step k , and $\Delta = [t_{k-1}, t_k]$. However, a key limitation of traditional SSMs lies in their Linear Time-Invariant (LTI) nature, where fixed parameters such as A, B, C , and Δ restrict their ability to adapt to diverse sequences. Mamba [39], a recent model developed based on SSMs, addresses this issue by introducing a selection mechanism that parameterizes these matrices as functions of the input x , enabling input-dependent dynamics. The parameterization is defined as

$$B \rightarrow S^B = W^B x, \quad (5)$$

$$C \rightarrow S^C = W^C x, \quad (6)$$

$$\Delta \rightarrow S^\Delta = \tau_\Delta \cdot \text{BroadCast}_D(W^\Delta x), \quad (7)$$

where W^B, W^C , and W^Δ are learnable projection matrices, τ_Δ is the softplus activation function, and BroadCast_D is a function that replicates the result of $W^\Delta x$ across all feature dimensions. This transition to a time-variant model allows Mamba to adaptively filter irrelevant information while retaining critical context, making it highly effective for tasks requiring long-context modeling [40].

III. THE MOEMBA FRAMEWORK

The proposed MoEMba framework is built based on the Mamba architecture, chosen for its efficient inference and ability to handle long sequences in light of its linear scaling with sequence length. MoEMba decodes muscle activity and recognizes gestures by establishing contextual dependencies across EMG signal channels. As depicted in Fig. 1, the architecture comprises of three key modules: (i) *WTFM Block*: This block is employed as a shallow feature extraction module to enhance multi-scale temporal representations; (ii) *MoE Block*: This block combines Mamba-based experts via sparse gating for dynamic pattern modelling; and (iii) *Classification Block*: A voting mechanism is used in the classification block to ensure robust signal-level predictions. Detailed description of each block is presented in the subsequent sub-sections.

A. The WTFM Block

In multivariate time series classification, particularly when dealing with high-dimensional data such as HD-sEMG signals, capturing both local temporal dynamics and global contextual information is crucial. In this regard and inspired by a recent work [41], we adopt a multi-scale representation learning through wavelet transform feature modulation. Such an approach enhances feature representation learning from HD-sEMG signals.

The MoEMba processes each signal patch, $P_i \in \mathbb{R}^{L \times V}$, by the WTFM block, where L defines the temporal length and V denotes the number of channels. This 2D representation facilitates convolutional operations, allowing a more effective capture of spatial relationships across channels. The WTFM block initially extracts local and global temporal features using small (e.g., 3×3) and large (e.g., 7×7) temporal convolutional kernels, respectively. A Discrete Wavelet Transform (DWT) is then applied to the local temporal features (extracted by the small temporal convolutional kernel), decomposing them into four directional components: approximation (c_A), horizontal detail (c_H), vertical detail (c_V), and diagonal detail (c_D). These components are calculated based on different frequency bands of the wavelet decomposition. These components capture detailed temporal variations at different scales. DWT components are then upsampled back to the original size of P_i using bicubic interpolation. These upsampled wavelet features are then refined using a channel attention mechanism, which learns to focus on the most important channels. The attention weights α_1 are given by

$$\alpha_1 = \sigma(W_2 \cdot \text{ReLU}(W_1 \cdot \text{MaxPool}(c_*^i))), \quad (8)$$

where W_1 and W_2 are learnable parameters, c_*^i refers to wavelet components (c_A^i, c_H^i, c_V^i , and c_D^i) associated with i^{th} patch. $\text{MaxPool}(\cdot)$ reduces the spatial dimensions, and $\sigma(\cdot)$ is

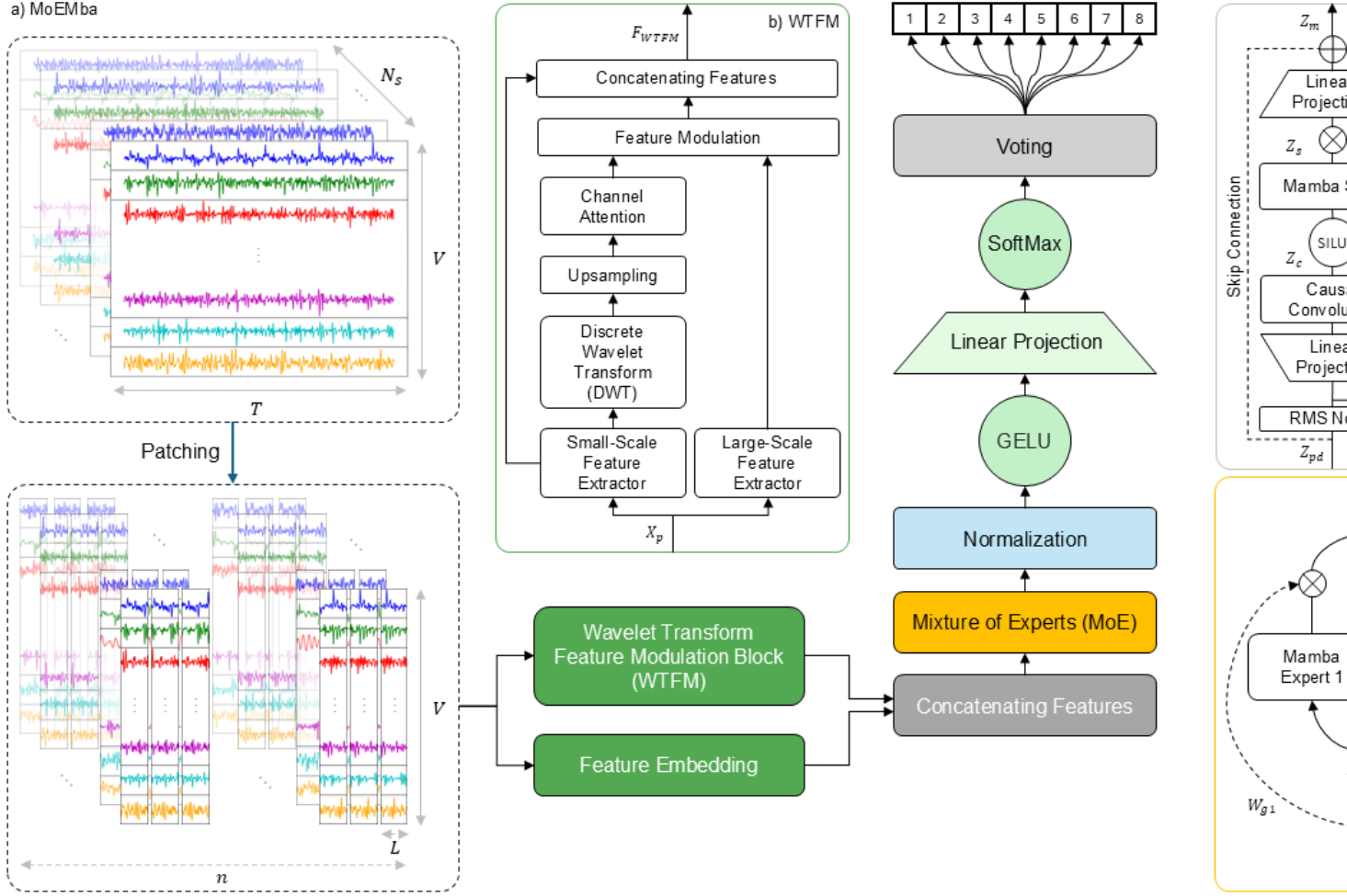


Fig. 1. MoEMba Framework. (a) Raw time series data is pre-processed via patching. (b) Shallow features are extracted using small (3×3) and large (7×7) receptive field convolutions, and wavelet transform-modulated features, with channel attention applied to EMG signal patches. (c) A Mixture of Experts (MoE) block routes patches to two Mamba experts based on a gating network. (d) The Mamba block incorporates projections, 1D convolution, selective State-Space Modeling (SSM), and skip connections for temporal dependency learning.

the sigmoid function. The enhanced wavelet features are then combined with the original large-scale features (extracted by the large temporal convolutional kernel) using a Hadamard product to capture both global and local information. This modulation process enhances the model's ability to discriminate subtle temporal patterns within the EMG signals while retaining crucial global information. After modulation, the refined large-scale features are concatenated with the small-scale features to integrate both high-level temporal representations and fine-grained local details. This fusion enables the model to utilize complementary information from different temporal scales, further improving its ability to capture intricate sEMG signal patterns. Finally, the combined feature set (F_{WTFM}) is fused with raw patch embeddings (F_{chan})—obtained via 1D convolutional value embedding function encapsulating the original signal's channel characteristics—to integrate both FD and TD information, improving encoder performance. The model backbone network then processes the fused features Z_p for deeper feature extraction.

$$Z_p = \text{Concat}(F_{WTFM}, F_{chan}), \text{ where } Z_p \in \mathbb{R}^{N_s \times n \times E \times V} \quad (9)$$

This completes description of the WTFM block of the proposed MoEMba framework. Next, we present the MoE module of the proposed MoEMba framework.

B. The MoE Block

The MoE block is utilized with each expert being implemented as a Mamba module. The MoE framework consists of a set of η experts (E_1, \dots, E_η), each specializing in learning distinct patterns within the time series data, and a gating network (G) that dynamically computes a sparse η -dimensional vector to weight the contributions of each expert. Given a sequence of embedded patches Z_p , the final output Z_θ is computed from the expert outputs as follows

$$Z_\theta = \sum_{i=1}^{\eta} G_i(Z_p) \cdot E_i(Z_p). \quad (10)$$

This formulation allows the MoE framework to adaptively combine the strengths of multiple Mamba experts, facilitating robust modeling of both short-term and long-term trends in hand gesture data.

We incorporate an adapted gating mechanism inspired by [28] that introduces optimizing enhanced sparsity to

optimize computational efficiency of the underlying model. More specifically, a tunable sparsity mechanism is employed where Gaussian noise, controlled by a trainable weight matrix W_{noise} , is added to the network output before applying the Softmax function. To further promote sparsity, only the top k values from the network output are retained, while the remaining values are suppressed to $-\infty$, effectively setting their corresponding gate values to zero. This selective approach is formalized as follows

$$\mathcal{G}(Z_p) = \text{Softmax}(\text{TopKGating}(H(Z_p), k)), \quad (11)$$

$$\text{where } H_i(Z_p) = (Z_p W_{\text{gate}})_i + \text{Softplus}((Z_p W_{\text{noise}})_i), \quad (12)$$

and $\text{TopKGating}(v, k)_i$ retains only the top k elements of v , setting the rest to $-\infty$. Here, W_{gate} and W_{noise} are trainable weight matrices. To prevent the potential bias in the gating network towards a single expert, a balanced gate mechanism is implemented. This is achieved by minimizing a balance loss \mathcal{L}_B , which encourages a more uniform distribution of samples across experts. The balance loss is defined as

$$\mathcal{L}_B(Z_p) = \lambda_B \cdot \text{CV}(\text{Load}(Z_p))^2, \quad (13)$$

where $\text{CV}(\cdot)$ is the coefficient of variation of the load vector, the Load function ($\text{Load}(\cdot)$) is a smooth estimator used to quantify the distribution of data samples across the different experts, and λ_B is a scaling factor. Additionally, a regularization term \mathcal{L}_Z has been used to penalize large logits within the network, further stabilizing the gating mechanism

$$\mathcal{L}_Z(Z_p) = \frac{1}{n} \sum_{i=1}^n \left(\log \sum_{j=1}^{\eta} e^{(Z_p)_j} \right)^2, \quad (14)$$

where n is the number of patches and η is the number of experts. The total auxiliary loss \mathcal{L}_{aux} is a weighted combination of these losses, integrated into the overall model loss function to ensure balanced and efficient expert utilization. Such a gating network allows to capture complex temporal dependencies in HD-sEMG signals.

C. Classification Block

The final stage of the MoEMba uses a classification head to process the MoE output, normalizing and activating it prior to projection into the class space. The resulting logits are then transformed into probabilities via softmax, and the predicted class is determined by selecting the highest probability. Afterwards, predictions from patches belonging to the same signal are aggregated, and majority voting is used to determine the final classification of the entire signal. This approach reduces the impact of noisy/inconsistent predictions at the patch level.

IV. EXPERIMENTAL RESULTS

In this section, we evaluate performance of the proposed MoEMba framework on the CapgMyo DB-b HD-sEMG datasets [30], and provide comparisons with baseline SOTA models. The primary objective is addressing the challenge of inter-session variability to have more consistent and generalizable performance, both within and between subjects. Single-trial EMG signals inherently suffer from a low

TABLE I
COMPARISON RESULTS USING THE DB-B DATASET.

Model	Author	Accuracy
TD	K. Englehart et al. [42]	0.416±0.198
ETD	R. N. Khushaba et al. [43]	0.437±0.209
NinaPro	M. Atzori et al. [44]	0.425±0.170
SampEn	A. Phinyomark et al. [45]	0.448±0.217
TVGGNet	J. Pereira et al. [29]	0.420±0.183
The Proposed MoEMba	This Work	0.569±0.201

Signal-to-Noise Ratio (SNR) and variability due to factors such as electrode placement, skin impedance, time of day, and participant conditions. Consequently, we evaluated the inter-session gesture recognition performance on the DB-b dataset, utilizing a train-on-one-session, test-on-the-other approach, while the DB-a dataset was incorporated for data augmentation during the training phase. However, due to data corruption in the final subject's recordings, the experiment proceeded with the first nine subjects in DB-b [29]. The model's gesture classification performance was then evaluated across eight distinct classes: "Thumb up," "Extension of index and middle with flexion of the others," "Flexion of ring and little finger with extension of the others," "Thumb opposing the base of the little finger," "Abduction of all fingers," "Fingers flexed together in a fist," "Pointing index," and "Adduction of extended fingers".

All experiments were conducted on a computing system equipped with an NVIDIA GeForce RTX 2080 Ti GPU, an Intel i9-9820X CPU, and 128GB of RAM. The MoEMba framework was configured with several key hyperparameters. The SSM employed a state expansion factor of 16 and a local convolution width of 4, with a model dimension of 128. The MoE architecture consisted of two experts and two gating networks, with a hidden dimension factor of 1. Each Mamba expert within the MoE framework used a block expansion factor of 4. A small number of experts was chosen to reduce the risk of overfitting, particularly given the dataset size, while ensuring that each expert receives sufficient data for effective training. The model was trained over 50 epochs, using a batch size of 32 and an initial learning rate of 0.0001, which was adjusted via a cosine annealing schedule.

Performance evaluation was conducted using three well-established classification metrics: total accuracy, confusion matrix, and Receiver Operating Characteristic (ROC) curves. Total accuracy was computed using a "winner-take-all" approach, measuring the percentage of correctly assigned labels. The confusion matrix provided a class-wise breakdown of correct classifications and false positive/negative rates. Given the eight-class setup, the resulting confusion matrix (Fig. 2 (a)) was 8×8 , where diagonal elements indicated correct classifications, while off-diagonal elements represented misclassifications. Additionally, the ROC curve (Fig. 2 (b)) is used to assess classification performance across varying thresholds, with the Area Under the Curve (AUC) serving as a summary measure of classifier effectiveness.

Table I summarizes the performance metrics of MoEMba

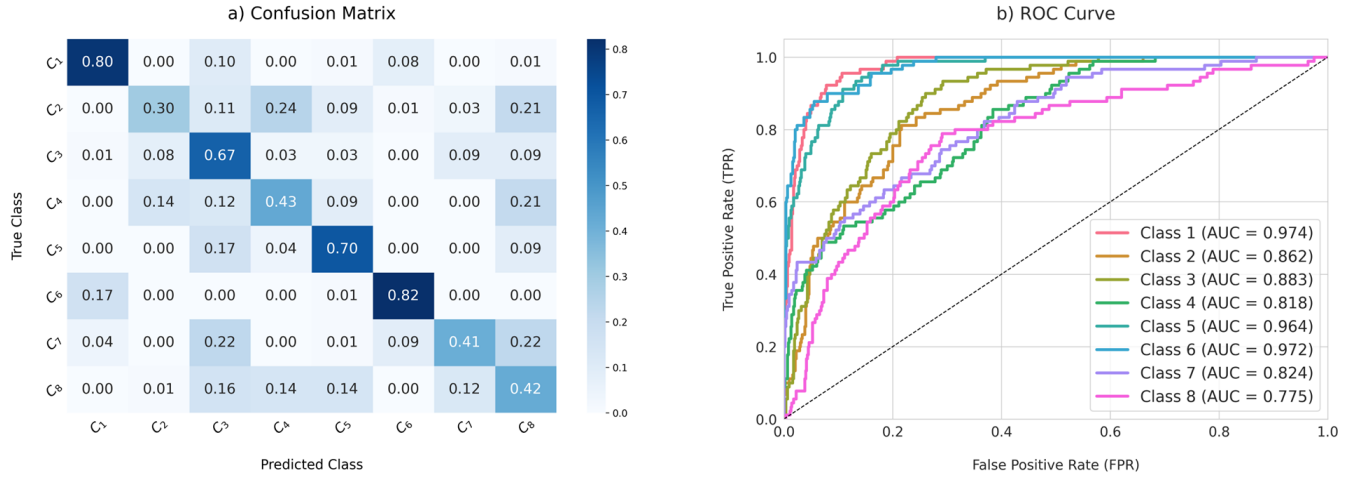


Fig. 2. Confusion Matrix and Receiver Operating Characteristic (ROC) Curves. (a) The heatmap visually represents the class-wise prediction probabilities within the primary dataset. The horizontal axis corresponds to predicted labels, while the vertical axis indicates true labels. Diagonal values reflect individual class accuracies, whereas off-diagonal values represent misclassification probabilities. Darker colors signify higher probabilities, while lighter shades indicate lower ones. The chance level is 0.125. (b) The ROC curves illustrate the classification performance of MoEMba across different discrimination thresholds. Each class is color-coded, with corresponding labels and the Area Under the ROC Curves (AUC) provided in the legend at the bottom right. The dashed black diagonal line represents random chance classification.

and its counterpart models. As the results highlight, MoEMba achieved a balanced accuracy of 56.9%, which is significantly above the random chance level of 12.5% for an eight-class problem. Notably, model comparisons revealed a trade-off between accuracy and network complexity, with the MoEMba framework achieving performance comparable to SOTA transformer-based architectures while maintaining substantially lower computational complexity. Unlike transformer models, which typically have quadratic complexity $O(n^2)$, MoEMba operates with linear complexity $O(n)$, making it well-suited for long time-series processing, such as sEMG signal classification.

The ROC analysis further illustrated class-specific performance, with AUC values of 0.974, 0.862, 0.883, 0.818, 0.964, 0.972, 0.824, and 0.775 across the eight gesture classes. The variation in classification accuracy can be attributed to differences in muscle activation patterns. Gestures such as “Thumb up” and “Abduction of all fingers” exhibited higher accuracy due to their distinct and easily recognizable muscle activation, whereas gestures involving partial flexion and extension, such as “Extension of index and middle with flexion of the others” and “Adduction of extended fingers,” were more prone to misclassification due to overlapping signal features. Moreover, inter-session variability, particularly changes in electrode placement and skin conditions, posed additional challenges in maintaining classification consistency.

Beyond accuracy, the computational efficiency of MoEMba underscores its potential for real-time applications. FLOPS is a key metric that quantifies the number of floating-point operations a system can perform per second, providing insight into the processing power required. The model’s lightweight architecture and compact design, with a total of 455,003 parameters and 27,312,144 FLOPS, enable efficient processing of long sequences while maintaining implementation feasibility. Furthermore, its streamlined architecture ensures scalability, allowing deployment

across various platforms without significant computational overhead. However, certain limitations remain, such as the need for larger training datasets to enhance generalization and the risk of overfitting when applied to smaller datasets.

V. CONCLUSION

In this study, we introduced the MoEMba framework, a novel approach for HD-sEMG-based hand gesture recognition, leveraging the Mamba architecture to address the critical challenge of session-to-session variability. Our experimental results demonstrated that the MoEMba framework achieves superior performance compared to its SOTA counterparts, with a balanced accuracy of 56.9% on the CapgMyo DB-b dataset. This performance is achieved while maintaining computational efficiency. The integration of wavelet feature modulation and channel attention mechanisms within the MoEMba framework enhances the model’s ability to capture both local and global temporal dependencies, leading to improved gesture recognition accuracy. Additionally, the MoE configuration allows the model to dynamically adapt to varying patterns in the HD-sEMG signals. A fruitful direction for future research is optimizing the model’s robustness to inter-session variability by exploring synthetic data to augment real-world datasets. Another direction for future research is to investigate the potential of incorporating additional modalities, to further improve the accuracy and reliability of gesture recognition systems.

REFERENCES

- [1] B. K. Hodossy, A. S. Guez, S. Jing, W. Huo, R. Vaidyanathan, and D. Farina, “Leveraging high-density emg to investigate bipolar electrode placement for gait prediction models,” *IEEE Transactions on Human-Machine Systems*, 2024.
- [2] M.-J. Hu, Y.-L. Gong, X.-J. Chen, and B. Han, “A gesture recognition method based on mic-attention-lstm,” *Hum.-Centric Comput. Inf. Sci.*, vol. 13, p. 21, 2023.

- [3] D. Farina, N. Jiang, H. Rehbaum, A. Holobar, B. Graimann, H. Dietl, and O. C. Aszmann, "The extraction of neural information from the surface emg for the control of upper-limb prostheses: emerging avenues and challenges," *IEEE Transactions on Neural Systems and Rehabilitation Engineering*, vol. 22, no. 4, pp. 797–809, 2014.
- [4] N. Parajuli, N. Sreenivasan, P. Bifulco, M. Cesarelli, S. Savino, V. Niola, D. Esposito, T. J. Hamilton, G. R. Naik, U. Gunawardana *et al.*, "Real-time emg based pattern recognition control for hand prostheses: A review on existing methods, challenges and future implementation," *Sensors*, vol. 19, no. 20, p. 4596, 2019.
- [5] A. Fleming, N. Stafford, S. Huang, X. Hu, D. P. Ferris, and H. H. Huang, "Myoelectric control of robotic lower limb prostheses: a review of electromyography interfaces, control paradigms, challenges and future directions," *Journal of neural engineering*, vol. 18, no. 4, p. 041004, 2021.
- [6] J. O. d. O. de Souza, M. D. Bloedow, F. C. Rubo, R. M. de Figueiredo, G. Pessin, and S. J. Rigo, "Investigation of different approaches to real-time control of prosthetic hands with electromyography signals," *IEEE Sensors Journal*, vol. 21, no. 18, pp. 20674–20684, 2021.
- [7] X. Lv, C. Dai, H. Liu, Y. Tian, L. Chen, Y. Lang, R. Tang, and J. He, "Gesture recognition based on semg using multi-attention mechanism for remote control," *Neural Computing and Applications*, vol. 35, no. 19, pp. 13839–13849, 2023.
- [8] K. M. Al-Aubidy and M. M. Abdulghani, "Towards intelligent control of electric wheelchairs for physically challenged people," *Advanced Systems for Biomedical Applications*, pp. 225–260, 2021.
- [9] H. Iqbal, J. Zheng, R. Chai, and S. Chandrasekaran, "Electric powered wheelchair control using user-independent classification methods based on surface electromyography signals," *Medical & Biological Engineering & Computing*, vol. 62, no. 1, pp. 167–182, 2024.
- [10] C. R. Carvalho, J. M. Fernández, A. J. Del-Ama, F. Oliveira Barroso, and J. C. Moreno, "Review of electromyography onset detection methods for real-time control of robotic exoskeletons," *Journal of neuroengineering and rehabilitation*, vol. 20, no. 1, p. 141, 2023.
- [11] J. R. Torres-Castillo, C. O. Lopez-Lopez, and M. A. Padilla-Castaneda, "Neuromuscular disorders detection through time-frequency analysis and classification of multi-muscular emg signals using hilbert-huang transform," *Biomedical Signal Processing and Control*, vol. 71, p. 103037, 2022.
- [12] U. Eraslan, A. Kitis, A. F. Demirkan, and R. H. Ozcan, "Effect of electromyographic biofeedback training on functional status in zone i-iii flexor tendon injuries: a randomized controlled trial," *Physiotherapy Theory and Practice*, vol. 39, no. 8, pp. 1563–1573, 2023.
- [13] H. Converse, T. Ferraro, D. Jean, L. Jones, V. Mendhiratta, E. Navias, M. Par, T. Rimlinger, S. Southall, J. Sprengle *et al.*, "An emg biofeedback device for video game use in forearm physiotherapy," in *SENSORS, 2013 IEEE*. IEEE, 2013, pp. 1–4.
- [14] S. Ni, M. A. Al-qaness, A. Hawbani, D. Al-Alimi, M. Abd Elaziz, and A. A. Ewees, "A survey on hand gesture recognition based on surface electromyography: Fundamentals, methods, applications, challenges and future trends," *Applied Soft Computing*, p. 112235, 2024.
- [15] D. Xiong, D. Zhang, X. Zhao, and Y. Zhao, "Deep learning for emg-based human-machine interaction: A review," *IEEE/CAA Journal of Automatica Sinica*, vol. 8, no. 3, pp. 512–533, 2021.
- [16] R. N. Khushaba, S. Kodagoda, M. Takruri, and G. Dissanayake, "Toward improved control of prosthetic fingers using surface electromyogram (emg) signals," *Expert Systems with Applications*, vol. 39, no. 12, pp. 10731–10738, 2012.
- [17] A. H. Al-Timemy, R. N. Khushaba, G. Bugmann, and J. Escudero, "Improving the performance against force variation of emg controlled multifunctional upper-limb prostheses for transradial amputees," *IEEE Transactions on Neural Systems and Rehabilitation Engineering*, vol. 24, no. 6, pp. 650–661, 2015.
- [18] S. Karheily, A. Moukadem, J.-B. Courbot, and D. O. Abdeslam, "semg time-frequency features for hand movements classification," *Expert Systems with Applications*, vol. 210, p. 118282, 2022.
- [19] X. Mian, Z. Bingtao, C. Shiqiang, and L. Song, "Mcmp-net: Mlp combining max pooling network for semg gesture recognition," *Biomedical Signal Processing and Control*, vol. 90, p. 105846, 2024.
- [20] W. Li, P. Shi, and H. Yu, "Gesture recognition using surface electromyography and deep learning for prostheses hand: state-of-the-art, challenges, and future," *Frontiers in neuroscience*, vol. 15, p. 621885, 2021.
- [21] E. Rahimian, S. Zabihi, S. F. Atashzar, A. Asif, and A. Mohammadi, "Surface emg-based hand gesture recognition via hybrid and dilated deep neural network architectures for neurobotic prostheses," *Journal of Medical Robotics Research*, vol. 5, no. 01n02, p. 2041001, 2020.
- [22] E. Tyacke, K. Gupta, J. Patel, R. Katoch, and S. F. Atashzar, "From unstable contacts to stable control: A deep learning paradigm for hd-semg in neurobotics," *arXiv preprint arXiv:2309.11086*, 2023.
- [23] T. Sun, Q. Hu, J. Libby, and S. F. Atashzar, "Deep heterogeneous dilation of lstm for transient-phase gesture prediction through high-density electromyography: Towards application in neurobotics," *IEEE Robotics and Automation Letters*, vol. 7, no. 2, pp. 2851–2858, 2022.
- [24] M. Jabbari, R. N. Khushaba, and K. Nazarpour, "Emg-based hand gesture classification with long short-term memory deep recurrent neural networks," in *2020 42nd Annual International Conference of the IEEE Engineering in Medicine & Biology Society (EMBC)*. IEEE, 2020, pp. 3302–3305.
- [25] C. Zeng, Z. Liu, G. Zheng, and L. Kong, "C-mamba: Channel correlation enhanced state space models for multivariate time series forecasting," *arXiv preprint arXiv:2406.05316*, 2024.
- [26] S. Zabihi, E. Rahimian, A. Asif, and A. Mohammadi, "Light-weight cnn-attention based architecture for hand gesture recognition via electromyography," in *ICASSP 2023-2023 IEEE International Conference on Acoustics, Speech and Signal Processing (ICASSP)*. IEEE, 2023, pp. 1–5.
- [27] M. Montazerin, E. Rahimian, F. Naderkhani, S. F. Atashzar, S. Yanushkevich, and A. Mohammadi, "Transformer-based hand gesture recognition from instantaneous to fused neural decomposition of high-density emg signals," *Scientific reports*, vol. 13, no. 1, p. 11000, 2023.
- [28] K. Alkilane, Y. He, and D.-H. Lee, "Mixmamba: Time series modeling with adaptive expertise," *Information Fusion*, vol. 112, p. 102589, 2024.
- [29] J. Pereira, D. Halatsis, B. Hodossy, and D. Farina, "Tackling electrode shift in gesture recognition with hd-emg electrode subsets," in *ICASSP 2024-2024 IEEE International Conference on Acoustics, Speech and Signal Processing (ICASSP)*. IEEE, 2024, pp. 1786–1790.
- [30] Y. Du, W. Jin, W. Wei, Y. Hu, and W. Geng, "Surface emg-based inter-session gesture recognition enhanced by deep domain adaptation," *Sensors*, vol. 17, no. 3, p. 458, 2017.
- [31] H. Li, Y. Li, J. Luo, X. Jiao, J. Liu, L. Zhou, L. Chang, and J. Zhou, "A high accuracy and real-time semg-based hand gesture classifier using lda-based template matching with adaptive majority vote and online data augmentation," *IEEE Sensors Journal*, 2024.
- [32] M. R. Islam, D. Massicotte, P. Massicotte, and W.-P. Zhu, "Surface emg-based inter-session/inter-subject gesture recognition by leveraging lightweight all-convnet and transfer learning," *IEEE Transactions on Instrumentation and Measurement*, 2024.
- [33] T. Xia, F. Wang, S. Kawata, J. Zhao, J. She, and D. Chugo, "Capturing spatial information for semg-based gesture recognition using graph attention networks," in *2024 IEEE Conference on Pervasive and Intelligent Computing (PICom)*. IEEE, 2024, pp. 137–141.
- [34] M. Emimal, W. J. Hans, T. Inbamalar, and N. M. Lindsay, "Classification of emg signals with cnn features and voting ensemble classifier," *Computer Methods in Biomechanics and Biomedical Engineering*, pp. 1–15, 2024.
- [35] J. Pereira, M. Alummoottil, D. Halatsis, and D. Farina, "Spatial adaptation layer: Interpretable domain adaptation for biosignal sensor array applications," *arXiv preprint arXiv:2409.08058*, 2024.
- [36] Y. Liu, T. Hu, H. Zhang, H. Wu, S. Wang, L. Ma, and M. Long, "itransformer: Inverted transformers are effective for time series forecasting," *arXiv preprint arXiv:2310.06625*, 2023.
- [37] Y. Nie, N. H. Nguyen, P. Sinthong, and J. Kalagnanam, "A time series is worth 64 words: Long-term forecasting with transformers," *arXiv preprint arXiv:2211.14730*, 2022.
- [38] A. Gu, K. Goel, and C. Ré, "Efficiently modeling long sequences with structured state spaces," *arXiv preprint arXiv:2111.00396*, 2021.
- [39] A. Gu and T. Dao, "Mamba: Linear-time sequence modeling with selective state spaces," *arXiv preprint arXiv:2312.00752*, 2023.
- [40] H. Qu, L. Ning, R. An, W. Fan, T. Derr, H. Liu, X. Xu, and Q. Li, "A survey of mamba," *arXiv preprint arXiv:2408.01129*, 2024.
- [41] Y. Huang, T. Miyazaki, X. Liu, and S. Omachi, "Irsrmamba: Infrared image super-resolution via mamba-based wavelet transform feature modulation model," *arXiv preprint arXiv:2405.09873*, 2024.
- [42] K. Englehart and B. Hudgins, "A robust, real-time control scheme for

- multifunction myoelectric control,” *IEEE transactions on biomedical engineering*, vol. 50, no. 7, pp. 848–854, 2003.
- [43] R. N. Khushaba and S. Kodagoda, “Electromyogram (emg) feature reduction using mutual components analysis for multifunction prosthetic fingers control,” in *2012 12th International Conference on Control Automation Robotics & Vision (ICARCV)*. IEEE, 2012, pp. 1534–1539.
- [44] M. Atzori, A. Gijsberts, C. Castellini, B. Caputo, A.-G. M. Hager, S. Elsig, G. Giatsidis, F. Bassetto, and H. Müller, “Electromyography data for non-invasive naturally-controlled robotic hand prostheses,” *Scientific data*, vol. 1, no. 1, pp. 1–13, 2014.
- [45] A. Phinyomark, F. Quaine, S. Charbonnier, C. Serviere, F. Tarpin-Bernard, and Y. Laurillau, “Emg feature evaluation for improving myoelectric pattern recognition robustness,” *Expert Systems with applications*, vol. 40, no. 12, pp. 4832–4840, 2013.